



On the notch sensitivity of cast iron under multi-axial fatigue loading

P. Livieri, E. Maggiolini, R. Tovo

University of Ferrara, Italy

paolo.livieri@unife.it, enrico.maggiolini@unife.it, roberto.tovo@unife.it

ABSTRACT. This work deals with the notch sensitivity of sharp notches under multi-axial fatigue loading. The main discussion concerns the differences in notch sensitivity at high cycle fatigue regime, between tensile, torsional and combined loading. For this comparison, this paper considers a large set of fatigue experimental tests and several computing simulations analyzed with several notch theories for predicting fatigue life of a component. The considered experimental data, taken from literature, deal with the fatigue behavior of cast iron circumferentially V-notched specimens under tension, torsion, and combined loading mode. This paper tries to apply several techniques for theoretical strength assessment and to compare different procedures. The examined procedures need the computation of many parameters, focusing on the importance of using the tensile resistance to set these parameters or using both tensile and torsion resistances. However, the improvements obtained by means of the more complex procedures are not noteworthy, compared to the overall scatter. In author's opinion, the differences in notch sensitivity under tensile and torsional loading remain questionable.

KEYWORDS. Notch; Fatigue; Tensile; Torsion; Combined load.

INTRODUCTION

The well-known problem of estimating the fatigue life of severely notched components, in the literature, is comprehensively studied, regardless of the material: for example carbon steel [1], titanium alloy [2] or polycrystals [3].

Since Neuber [4], the fatigue strength of notched components has been related not strictly to the peak stress at the notch tip, but to an effective stress defined as an average value over a small volume of material of depth “q”, depending on material. The difference between the increment of the peak stress and the actual reduction of strength at notches is usually called “notch sensitivity”.

Successively, for the “notch sensitivity” modelling, Peterson [5] largely confirmed the need of introducing at least one length, material dependent, to be compared with the notch tip radius.

Another way, to predict fatigue life of notched components, is obviously to perform several tests to build, for example, the SN diagram, but this strategy needs a lot of time and money.

Multi-axial fatigue tests on notched specimen has been performed and reported in different papers and conferences: in the presence of blunt circumferential notch [6], near holes [7], considering the crack behavior [8], under proportional/non-proportional loading [9]. It is possible to note the difference in the fatigue resistance by changing the loading mode, in the presence of geometrical irregularities. It was demonstrated by the Modified Wohler Curve Method the important role of



the shear stress in the stage I fatigue cracks [10] and of the normal stress that open and close the micro cracks influencing the propagation of themselves [11].

Anyway, even if the multi-axial notch sensitivity is a well-known global problem, its actual relationship with the load case is not definitely clear.

By taking advantage from the numerical tools, a simple strategy would be to investigate how the stress field is setup around the notch tip and to compute, by a FEM software or formulas, the fatigue strength according to the overall stress field at the notch tip and in the surrounding zone. Many procedures in the last years came up to provide for this problem (implicit gradient [12], critical distance [13], strain energy density [14] for instance) and many researchers are studying the way to predict the resistance of a notched component without specific experimental tests. One or more characteristic lengths lead all these theories.

These lengths are calibrated on reference cases: for instance, the pure tensile and torsion tests; but, is it necessary to study all the different cases? What about the load ratio? Is the combined in phase/out-of-phase test influenced by the pure torsion sensitivity or tensile strength knowledge is sufficient?

From applicative point of view, every current influencing factor requires a model and usually the introduction of a specific coefficient to be evaluated; at least one further undetermined coefficient should be fitted for every influencing factor introduced.

The paper investigates whether the loading mode is an actual influencing factor for the notch sensitivity of metals, i.e. if and how much it is necessary to change or modify the notch sensitivity assessment when uniaxial, or biaxial stress are applied to a notch.

In this paper, the investigation focuses on cast iron. Cast iron are expected to be more used in the next years, the production mechanism is improving the quality and cast iron has, by now, a good mechanical and technological properties. Many studies made on wind turbine [15-18] demonstrate the importance of casting thickness and microstructure in the fatigue mechanism. Metallurgical defects are inevitable and defects are very common especially on this kind of materials: cavities, porosity, graphite degenerated and so on; all of these imperfections influence the resistance of cast iron because this kind of defect could be compared to cracks [19]. Tests on sharp notches are particularly suitable because notches give to the designer the same problems of cracks, so tests on notches provide information concerning both notch sensitivity and defect tolerance of a material.

The aim of this paper is to understand the difference between setting the characteristic length only on the pure tensile test and setting on the pure tensile and on torsion resistance. For this purpose, the paper takes the fatigue strength of cast iron specimens under tensile, torsion and mixed in-phase and out-of-phase combined load from [20] and it compares the possible expectations computed by means of different theories.

THEORETICAL OVERVIEW OF NOTCH STRENGTH THEORIES

In the literature, it is simple to find out that, traditionally, almost all the theories usually are set up in pure tensile load case because tensile loading is the most common applied load, tensile is the most representative resistance and it is the most simple load to apply by testing devices. One of these approaches, for instance, is the Implicit Gradient.

Implicit gradient (IG)

This method, as proposed in [21], is particularly suitable for a numerical estimation of the component fatigue life dependent on its geometry; the idea is very simple and it enables the application of the average damage originally formulated in the 1930s by Neuber [4].

IG method is based on the assumption that the damage should be related to the average of the stress components occurring on the body, where the values near to the critical point are more important than the far away field. The influence zone dimension is regulated simply by the material properties and is indicated by the length ϵ .

In a body of volume V , it is possible to define a non-local effective tension σ_{eff} in a generic point x as an integral average of an equivalent local tension σ_{eq} , weighted by a Gaussian function $\psi(x,y)$ depending on the distance between points x and y of the body:

$$\sigma_{\text{eff,int}}(x) = \frac{1}{Vr(x)} \int_V \psi(x,y) \sigma_{\text{eq}}(y) dy = \frac{\int_V \psi(x,y) \sigma_{\text{eq}}(y) dV}{\int_V \psi(x,y) dV} \quad \text{in } V \quad (1)$$

where



$$\psi = \frac{e^{-\frac{|x-y|^2}{2L^2}}}{2L^2} \quad [\text{mm}^{-2}] \quad L=c\sqrt{2} \quad [\text{mm}] \quad (2)$$

By approximating Eq. (1), it is possible to define an effective stress σ_{eff} by the Helmholtz equation [22] using Neumann boundary conditions ($\nabla \sigma_{\text{eff}} \cdot \mathbf{n} = 0$) [4].

$$\sigma_{\text{eff,IG}} - c^2 \nabla^2 \sigma_{\text{eff,IG}} = \sigma_{\text{eq}} \quad \text{in } V \quad (3)$$

where σ_{eq} is the first principal stress (for example) and c is a material coefficient (for instance, it is 0.2 mm for weldable construction steel).

Theory of critical distance (TCD)

Another simple approach is the Critical Distance approach. In its original formulation the Critical Length is simply defined as a material characteristic length L , computed according to tensile properties of material:

$$L = \frac{1}{\pi} \left(\frac{\Delta K_{I,\text{th}}}{\Delta \sigma_A} \right) \quad (4)$$

The effective value of the stress is obtained by considering the elastic field around the notch tip. In particular the remarkable elastic stress field around the notch is obtained plotting the stress (i.e. the maximum principal stress) depending by the distance from the notch tip in a defined direction.

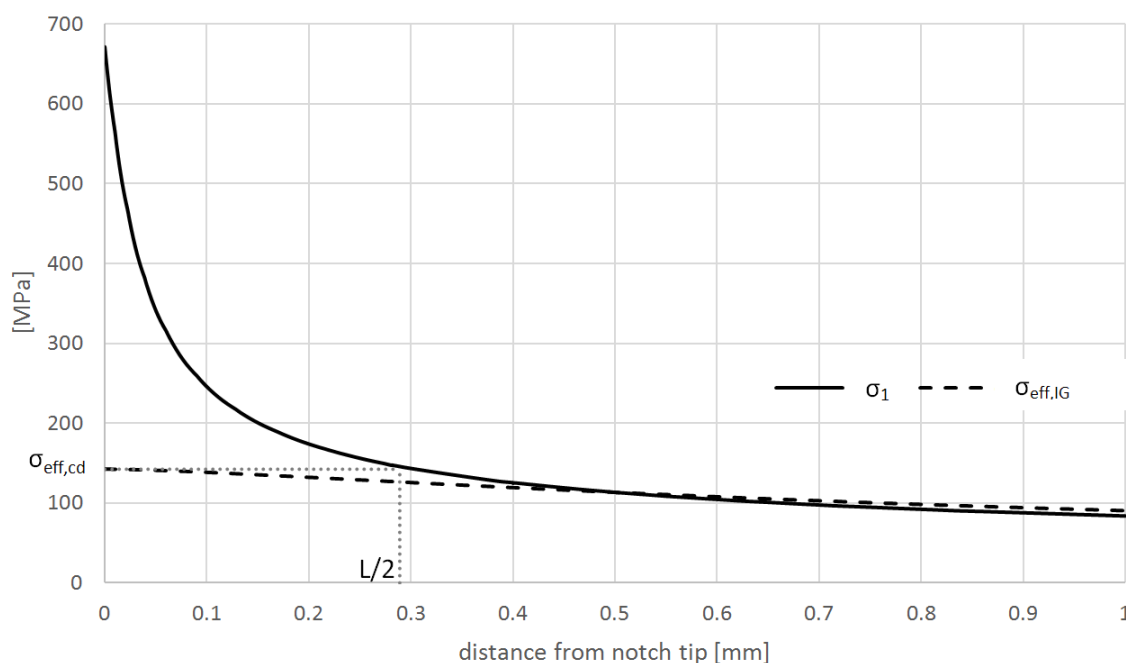


Figure 1: Stress distribution from a notch tip and effective values of CD and IG approaches.

Specifically, the point method states that the effective stress is the stress evaluated at one half of the critical length:

$$\sigma_{\text{eff,cd}} = \sigma_{\text{eq}}(L/2) \quad (5)$$

Having L given by material, the σ_{eff} can be easily found by the formulas or graphs similar to fig. 1.

Differently from the original formulation, in the case of combined loading, in the multi-axial fatigue [23, 24] a more general approach is proposed by suggesting a critical length linearly dependent from the biaxiality ratio ρ . The biaxiality ratio is defined by:



$$\varrho = - \frac{\sigma_3}{\sigma_1} \tag{6}$$

and consequently the critical length L depends from the biaxiality ratio according to:

$$L = a \varrho + b \tag{7}$$

In the above linear relationship, a and b are material constants to be determined by the critical distance value generated under two different ϱ ratios: for instance, Eq. (7) could be easily calibrated by considering the material characteristic length generated both under plane stress mode I loading ($\varrho = 0$) and under mode III loading ($\varrho = 1$).

We will call this linear variability of the critical length: “bi-parametric approach”, since its definition requires the calibration of the two values under separated loading conditions

Bi-parametric extension of the Implicit gradient (IG)

It is quite easy to provide a bi-parametric version of the Implicit Gradient approach too and such extension is here proposed.

By using the same linear dependence of Eq. (7), even the constant c of Eq. (3) can change according to the biaxiality ratio. Hence, in a bi-parametric version of the Implicit Gradient approach, c will be computed according to:

$$c = a' \varrho + b' \tag{8}$$

where, similarly to the Critical distance approach, a' and b' will be calibrated by means of two experimental values obtained under different biaxiality ratios.

Strain energy density (SED)

The energy stored in a body due to the deformation is called strain energy. The strain energy per volume unit is the SED, that is the area underneath the stress-strain curve up to the point of deformation. It is obvious that any strain energy density approach strictly speaking cannot be used at the tip of a sharp V-shaped notch since not only do stresses tend toward infinite (both in the case in which they obey the linear elasticity, and when they obey a power-hardening law), but so does the strain energy density. On the contrary, in a small but finite volume of material close to the notch, whichever its characteristics (blunt notch, severe notch, re-entrant corner, crack), the energy always has a finite value and the main question is rather that of estimating the size of this volume.

To calculate the SED in a finite volume around the focus point it needs:

- mode x eigenvalues, according to the Williams’ solution λ_x
- non dimensional shape factors in the NSIF expressions $k_{1,3}$
- V-notch depth $d^2=(D/2)-d$
- parameters for the energy density evaluation $e_{1,3}$
- poisson ratio ν
- young module E
- weight function c_w

The reference [20] demonstrates how to calculate the SED, at sharp notches, in a multi-axial case and for the specific experimental data considered in the following. The first point is the evaluation of the Notch SIF:

$$\Delta K_1 = k_1 d^{(1-\lambda_1)} \Delta \sigma_{nom} \tag{9}$$

$$\Delta K_3 = k_3 d^{(1-\lambda_3)} \Delta \tau_{nom} \tag{10}$$

Then, the radius of integration shall be evaluated, by obtaining two different values for tensile and torsional loading, i.e. mode I and III respectively.

$$R_1 = \left(\sqrt{2e_1} \frac{\Delta K_{1\Lambda}}{\Delta \sigma_{1\Lambda}} \right)^{\frac{1}{1-\lambda_1}} \tag{11}$$

$$R_3 = \left(\sqrt{\frac{e_3}{1+\nu}} \frac{\Delta K_{3\Lambda}}{\Delta \sigma_{3\Lambda}} \right)^{\frac{1}{1-\lambda_3}} \tag{12}$$

Finally, the effective Strain Energy Density shall be evaluated, by computing the average energy and by introducing an appropriate correction c_w due to the load ratio.

$$\overline{\Delta W} = \frac{1}{E} \left[e_1 \frac{\Delta K_1^2}{R_1^{2(1-\lambda_1)}} + e_3 \frac{\Delta K_3^2}{R_3^{2(1-\lambda_3)}} \right] \quad (13)$$

$$c_w = \begin{cases} \frac{1+R^2}{(1-R)^2} & \text{for } -1 \leq R < 0 \\ 1 & \text{for } R = 0 \\ \frac{1-R^2}{(1-R)^2} & \text{for } 0 < R \leq 1 \end{cases} \quad (14)$$

$$SED = c_w \overline{\Delta W} \quad (15)$$

Note that, since the integration fields are different under tensile and torsional loading and the two strengths shall be known for the SED evaluation, the proposed approach is actually a bi-parametric one.

A mono-parametric version of such theory can be easily obtained by using only the parameters evaluated under tensile loading; i.e. using only R_1 and assuming, for a sake of simplicity, R_3 equal to R_1 . This choice is not suggested in [20], but it is here introduced just for this specific investigation.

EXPERIMENTAL DATA FROM THE LITERATURE

For a discussion on real data, experimental tests taken from literature are here considered. Data are taken from the recent paper [20] previously cited and such experimental data concern the fatigue tests on sharp notches, made of ductile cast iron, under multi-axial loading. Cylindrical specimens are made of EN-GJS400 cast iron with a circumferential V-notch.

According to [20], the mechanical properties of the parent material are: $Y_S = 267$ MPa, $U_{TS} = 378$ MPa and the Elongation to fracture equal to 11.5%. The reference fatigue strength of the parent material, under fully reversed, tensile and under torsional loading, are $\sigma_A = 150.4$ MPa, $\tau_A = 145.6$ MPa.

The notched specimens were tested under tensile, torsion, mixed in phase and out-of-phase fatigue loading. The main results are in Tab. 2. Tab. 2 shows the following parameters: R = Stress ratio; λ = nominal biaxiality ratio; φ = phase shift angle under combined loading. The Tab. 2 provides, as an index of the obtained results, the values σ_A and τ_A , i.e. the average strength at 2 millions of cycles to failure for the considered case.

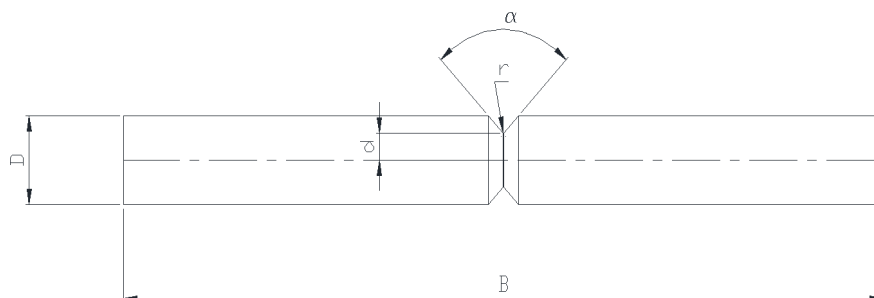


Figure 2: Geometry of experimental specimens [20].

B [mm]	D [mm]	d[mm]	α [°]	r [mm]
200	20	6	90	0.1

Tab. 1: Specimens size.



Data Set	R	Load case	phase shift angle φ	biaxiality ratio λ	σ_A [MPa]	τ_A [MPa]
A	-1	tension			89.9	
B	-1	torsion				151.9
C	-1	combined	0	1	74.0	74.0
D	-1	combined	90	1	82.6	82.6
E	-1	combined	90	0.6	85.9	51.5
F	-1	combined	0	0.6	99.7	59.8
G	0	tension			57.5	
H	0	torsion				109.5
I	0	combined	0	1	56.4	56.4
J	0	combined	90	1	53.3	53.3

Table 2: Results taken from [20].

NUMERICAL SIMULATIONS

The proposed approaches are based on the linear elastic stress field. Several FE tools can easily compute the linear elastic stress field. In the following, Comsol multiphysics FE software has been used because it is the easiest way to solve the Helmholtz equation Eq. (3), necessary for IG, due to the built-in PD equation solver. Authors developed another way to solve the IG with others FE software [25], but it turns out approximate and a direct solution is more accurate. TCD and SED do not need any specific software to be solved. A free mesh was applied on the most part of the geometry; a mapped mesh was used in the proximity of the notch tip. The investigated geometry has a tensile stress concentration factor $K_{t,\sigma}$ and the torsional stress concentration factor $K_{t,\tau}$ respectively equal to $K_{t,\sigma} = 7.467$ and $K_{t,\tau} = 3.178$.

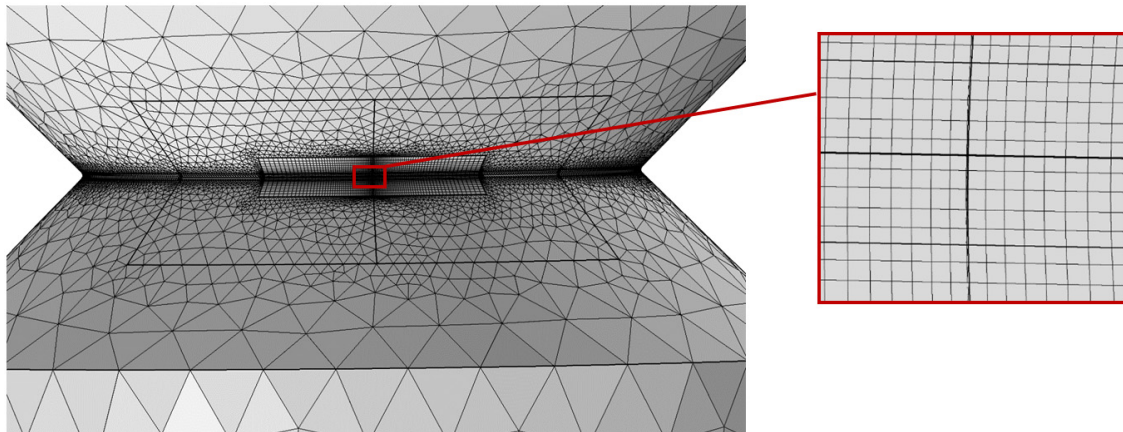


Figure 3: mapped mesh on the notch tip (element size= $r/6.25$).

APPLICATION OF EFFECTIVE STRESS THEORIES

For the actual computation of the effective values, according to presented theories, some further descriptions are necessary. First, an equivalent stress value shall be chosen for IG and CD approaches, see Eq. (3) and (5).



In [26], a large investigation has been carried out on a similar ductile cast iron. The main principal stress amplitude $\sigma_{1,a}$ turned out to be a proper choice for the equivalent stress under multi-axial fatigue loading. This choice will be adopted in the following.

Moreover, [26] demonstrated a large sensitivity to the mean principal stress value. In that case, a proper correction for the loading conditions with mean value different from zero, was the following:

$$\sigma_{eq,a} = \sigma_{1,a} + 0.5 \sigma_{1,m} \tag{16}$$

where $\sigma_{1,m}$ is the mean value of the main principal stress.

To characterize the length useful to calculate the effective stress, by using both tensile and torsion, we use the formula (7) for all the proposed techniques. The biaxility index Q is calculated with the nominal principal stresses values.

IG

According to previous equations and the given experimental data, the parameter “c” for the IG approach have been fitted on the pure tensile and torsional reverse loading: data set A and B of Tab. 2. They turn out to be $c_\sigma = 0.3985$ and $c_\tau = 0.5684$.

In a simple mono-parametric investigation “c” of Eq. (3) will be constant and equal to c_σ . In the case of a bi-parametric study, the characteristic length is a combination of tensile and torsion; according to the linear assumption of Eq. (7), it turns out to be:

$$c = (c_\tau - c_\sigma) * Q + c_\sigma \tag{17}$$

Obtained results are shown in Tab. 3. Note that, a perfect agreement of the proposed approach is obtained when the effective stress of the considered case is equal to the reference strength of the parent material under tensile loading, $\sigma_A = 150.4$ MPa.

R	Load case	σ_{nom}	τ_{nom}	$\sigma_{eff,GI}$ mono-par.	$\sigma_{eff,GI}$ bi-par.
-1	tensile	89.9	0.0	149.5	149.5
-1	torsion	0.0	151.9	169.2	144.5
-1	$\varphi=0^\circ \lambda=1$	74.0	74.0	174.9	163.2
-1	$\varphi=0^\circ \lambda=0.6$	99.7	59.8	198.0	190.0
-1	$\varphi=90^\circ \lambda=1$	82.6	82.6	125.8	128.0
-1	$\varphi=90^\circ \lambda=0.6$	85.8	51.5	130.8	125.2
0	tensile	57.6	0.0	143.7	143.7
0	torsion	0.0	109.6	183.1	156.4
0	$\varphi=0^\circ \lambda=1$	56.4	56.4	200.0	186.6
0	$\varphi=90^\circ \lambda=1$	53.3	53.3	152.1	141.9

Table 3: Effective stress values provided by the IG approach.

TCD

Similarly, to the IG approach, in the TCD methods, the critical length value have been fitted on tensile and torsional loading cases. The obtained values are: $L(\sigma) = 0.540$ mm and $L(\tau) = 0.968$ mm. For the dependence of L by combined tensile and torsion the Eq. (7) is used with $a=0.428$ and $b=0.540$. Results are shown in tab. 4



R	Load case	σ_{nom}	τ_{nom}	$\sigma_{eff,CD}$ mono-par.	$\sigma_{eff,CD}$ bi-par.
-1	tensile	89.9	0.0	149.9	149.9
-1	torsion	0.0	151.9	190.9	150.2
-1	$\varphi=0^\circ \lambda=1$	73.99	73.99	192.5	171.8
-1	$\varphi=0^\circ \lambda=0.6$	99.70	59.82	212.8	198.4
-1	$\varphi=90^\circ \lambda=1$	82.57	82.57	137.7	122.0
-1	$\varphi=90^\circ \lambda=0.6$	85.83	51.50	143.1	133.4
0	tensile	57.60	0.00	144.0	144.1
0	torsion	0.00	109.60	206.7	162.5
0	$\varphi=0^\circ \lambda=1$	56.40	56.40	220.2	196.4
0	$\varphi=90^\circ \lambda=1$	53.30	53.30	176.7	143.5

Table 4: Effective stress values provided by the CD approach.

SED

in order to apply the sed approach and to calculate the reference strength ΔK_A necessary for Eq. (11, 12), a possibility is to use the same reference tensile and torsional strength previously reported and used for the other approaches. from Eq. (11, 12) the integration field dimensions resulted respectively $r_1 = 0.48$ mm and $r_3 = 1.18$ mm. these results were one of the possibilities given by [20]; anyway, it is necessary to remark that the authors in [20] suggested even a slightly different choice by obtaining a lower r_1 radius equal to 0.33 mm.

in the following, we will use the final value suggested by the authors of [20].

however, this choice affects the absolute value of the results; but, in the following, the absolute comparison between different approaches could be questionable in any case and the main target of the following discussion will not be the absolute comparison of the proposed methods, but only the relative effect of the introduction of the bi-parametric sensitivity. so, at this stage, the actual r_1 used is not critical, if the choice is among the values proposed by the authors of [20]. In order to consider the characteristic length only depending by the tensile loading, i.e. the mono-parametric approach instead of the bi-parametric one, it is sufficient to set $r_3 = r_1 = 0.33$ mm.

having these data, it is simple to calculate sed and results are given in Tab. 5.

R	Load case	$\Delta\sigma_{nom 1}$	$\Delta\sigma_{nom 3}$	SED mono-par.	SED bi-par.
-1	tensile	179.8	0.0	0.152	0.152
-1	torsion	0.0	303.8	0.669	0.370
-1	$\varphi=0^\circ \lambda=1$	148.0	148.0	0.262	0.191
-1	$\varphi=0^\circ \lambda=0.6$	199.4	119.6	0.291	0.244
-1	$\varphi=90^\circ \lambda=1$	165.1	165.1	0.326	0.237
-1	$\varphi=90^\circ \lambda=0.6$	171.7	103.0	0.215	0.181
0	tensile	115.2	0.0	0.125	0.125
0	torsion	0.0	219.2	0.697	0.385
0	$\varphi=0^\circ \lambda=1$	112.8	112.8	0.304	0.221
0	$\varphi=90^\circ \lambda=1$	106.6	106.6	0.272	0.198

Table 5: SED values for the considered tests.

DISCUSSION

A first check of the obtained results could be a general overview of the overall accuracy. As previously stated, a good assessment is obtained when the effective stress values (or the SED), calculated at the reference strength (i.e. the values given in the previous tables) are the same for all the considered experimental test data. In this case, considered approaches have been fitted mainly on the tensile fully reversed loading test, hence the referring case is the set A of Tab. 2: tensile loading at $R = -1$.

For the considered approaches, this optimal condition is not completely satisfied. The scatter of the effective values is much lower than the nominal or peak values, but it is important. The combined loading conditions seem the most critical; there is an under estimation of the fatigue strength for the in-phase loading (because the effective values at the experimental strength value are higher than expected) and an over estimation of the fatigue strength for the out-of-phase loading, independently from the load ratio R .

For a quantitative comparison, the relative errors are defined as the effective value minus the referring tensile case (i.e. 150.4 MPa for stress) divided by the same strength. For the SED approach, errors have been computed on the squared roots of the obtained values, because SED is an energy and not a stress; elsewhere errors of the SED approach should be incorrectly too high compared to errors defined on stress values. A diagram of the obtained values is given in fig. 4.

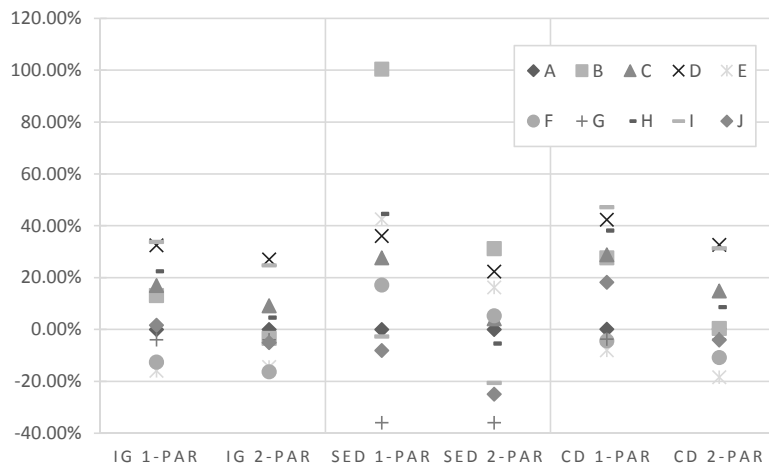


Figure 4: relative errors of obtained results.

A “box and whisker plot” can give a more appropriate representation of the scatter of the obtained results. Fig 5 shows the results. As usual, in this “boxplot” the bottom and the top of the boxes are the first and third quartiles, and the band inside the boxes is the second quartile (the median); the ends of the whiskers are the minimum and maximum of all of the data.

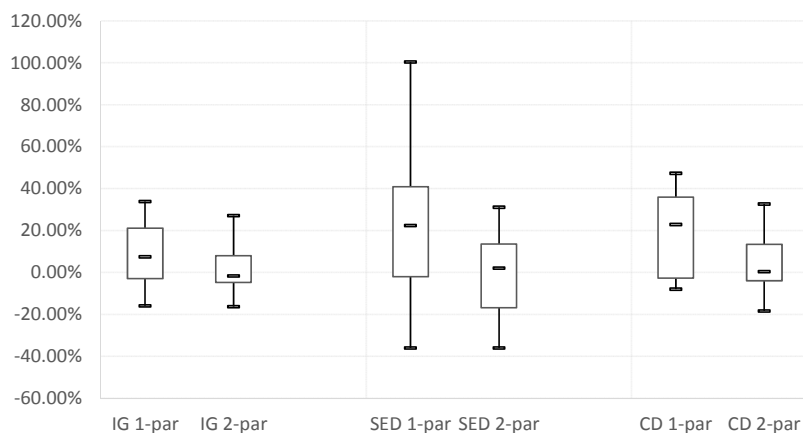


Figure 5: Box-plot of relative errors.



Apparently, mono-parametrical SED has a higher scatter; but it is not here proposed as an actual prediction procedure, it is simply here computed for the specific target of this paper. In this discussion, the main question does not deal with a comparison among the different approaches, but we want to comment the differences between the mono-parametric and the bi-parametric version of each approach.

It is clear that the median and the mean value of the bi-parametric approaches are better. In addition, the overall scatters are smaller; hence, we can say that the bi-parametric approaches are somehow better than the mono-parametric ones.

On the other hand, we can also say that this evidence is trivial, because bi-parametric approaches are fitted on two set of data, hence they shall necessary have a better outcome than the approaches fitted on just one set of data.

In our opinion, the problem turns out to be: is the obtained improvement actually significant compared to the overall scatter of the results?

The Analysis of Variance (ANOVA) can address this problem. The hypothesis to be verified is the equality of the mean response of the bi-parametric and the mono-parametric estimations, for each approach separately. The “null hypothesis” is the equality of the means; hence, the null hypothesis is that mono and bi-parametric estimations have equal mean values. Conversely, if we prove the inconsistency of the null hypothesis, we can say that the two estimations have actually different mean values and so they are substantially different.

By using the ANOVA, we make some questionable assumption; for instance, we accept that each estimation can be assumed as a random independent observation.

Tab. 6 gives the obtained values of the inconsistency of probability of the null hypothesis.

IG	SED	CD
62.3%	88.9%	86.8%

Table 6: Probability of inconsistency of the means equality obtained by the ANOVA.

Such probabilities of inconsistency of the null hypothesis are usually compared with an assumed confidence probability level, conventionally 95%, sometimes 90%. Each obtained value is lower than any usual confidence level; we have to conclude that, in the considered experimental data, the null hypothesis cannot be rejected. From a statistical point of view, it is not possible to state that means are actually different.

From an engineering point of view, we argue that the improvement of the bi-parametric approaches compared to the mono-parametric ones is not so substantial compared to the intrinsic scatter of the problem.

CONCLUSIONS

Three separate approaches for fatigue strength assessment of notches have been considered.

For each approach, two versions have been proposed: a first one, called mono-parametric, is defined by assuming the same notch sensitivity under tensile and torsion loading. In a second version, called bi-parametric, the notch sensitivity is different by changing the loading mode and the sensitivities under tensile and torsional loading are consequently different.

The obtained approaches have been tested on experimental data taken from the literature and dealing with the fatigue strength of sharp notches on a ductile cast iron.

The results have been statistically investigated by means of ANOVA too.

The main evidence is that the advantage of using bi-parametric approaches is not so convenient compared to the scatter of the problem, hence the different notch sensitivity under torsional loading is not clear and it is dependent on the chosen effective stress definition.

REFERENCES

- [1] Atzori, B., Berto, F., Lazzarin, P., Quaresimin, M., Multi-axial fatigue behaviour of a severely notched carbon steel, *International Journal of Fatigue*, 28 (2006) 485–493.



- [2] Wang, X.M., Cao, W., Deng, C.H., Liu, H., Pfetzinger-Micklich, J., Yue, Z.F., The effect of notches on the fatigue behavior in NiTi shape memory alloys, *Materials Science and Engineering A*, 610 (2014) 188–196.
- [3] Wan, V.V.C., MacLachlan, D.W., Dunne, F.P.E., A stored energy criterion for fatigue crack nucleation in polycrystals, *International Journal of Fatigue*, 68 (2014) 90-102.
- [4] Neuber, H., Über die Berücksichtigung der Spannungskonzentration bei Festigkeitsberechnungen. *Konstruktion*, 20 (7) (1968) 245-251.
- [5] Peterson, R.E., Notch sensitivity, In: *Metal Fatigue* (edited by G. Sines and J.L. Waisman), McGraw Hill, New York, (1959) 293-306.
- [6] Berto, F., Lazzarin, P., Marangon, C., Fatigue strength of notched specimens made of 40CrMoV13.9 under multiaxial loading”, *Materials and Design*, 54 (2014) 57–66.
- [7] Gates, N., Fatemi, A., Notched fatigue behavior and stress analysis under multiaxial states of stress, *International Journal of Fatigue*, 67 (2014) 2–14.
- [8] Matsubara, G., Nishio, K., Multiaxial high-cycle fatigue criterion for notches and superficial small holes from considerations of crack initiation and non-propagation, *International Journal of Fatigue*, 67 (2014) 28–37.
- [9] Chen, H., Shang, D.-G., Tian, Y.-J., Xu, G.-W., Multiaxial fatigue life prediction for notched components under proportional and non-proportional cyclic loading, *Applied Mechanics and Materials*, 197 (2012) 585-589.
- [10] Susmel, L., *Multiaxial notch fatigue from nominal to local stress-strain quantities.*, Cambridge, UK Woodhead & CRC; (2009).
- [11] Kanazawa, K., Miller, K.J., Brown, M.W., Low-cycle fatigue under out-of-phase loading conditions., *Trans ASME, J Eng Mater. Technol.*, (1977) 222–228.
- [12] [1]Tovo, R., Livieri, P., An implicit gradient application to fatigue of sharp notches and weldments, *Engineering Fracture Mechanics*, 74(4) (2007) 515-526.
- [13] Susmel, L., Taylor, D., The Theory of Critical Distances to estimate lifetime of notched components subjected to variable amplitude uniaxial fatigue loading, *International Journal of Fatigue*, 33(7) (2011) 900-911.
- [14] Lazzarin, P., Zambardi, R., A finite-volume-energy based approach to predict the static and fatigue behavior of components with sharp V-shaped notches, *International Journal of Fracture*, 112(3) (2001) 275-298.
- [15] Shirani, M., Härkegård, G., Casting defects and fatigue behaviour of ductile cast iron for wind turbine components: A comprehensive study, *Materialwissenschaft-und-Werkstofftechnik* (2011).
- [16] Shirani, M., Härkegård, G., Large scale axial fatigue testing of ductile cast iron for heavy section wind turbine components, *Engineering Failure Analysis*, 18 (2011) 1496–1510.
- [17] Roedter, H., Gagne, M., Ductile iron for heavy section wind mill castings a european experience., In: *Proceedings of the 2003 Keith D. Millis world symposium on ductile iron*, South Carolina, (2003) 11.
- [18] Shirani, M., Härkegård, G., Fatigue life distribution and size effect in ductile cast iron for wind turbine components., *Eng Fail Anal*, 18(1) (2011) 12-24.
- [19] Zambrano, H. R., Harkegard G., Stark, K. F., Fracture toughness and growth of short and long fatigue cracks in ductile cast iron EN-GJS-400-18-LT , *Fatigue and Fracture of Engineering Materials & Structures*, 35(4) (2012) 374-388
- [20] Berto, F., Lazzarin, P., Tovo, R., Multiaxial fatigue strength of severely notched cast iron specimens, *International Journal of Fatigue*, 67 (2014) 15–27.
- [21] Maggiolini, E., Livieri, P., Tovo, R., On numerical integration for effective stress assessment at notches, *Frattura ed Integrità Strutturale*, 25 (2013) 117-123; doi: 10.3221/IGF-ESIS.25.17.
- [22] Peerlings, R.H.J., de Borst, R., Brekelmans, W.A.M., de Vree, J.H.P., Gradient enhanced damage for quasi brittle material, *International Journal of Numerical Methods in Engineering*, 39 (1996) 3391–3403.
- [23] Susmel, L., Taylor, D., The Theory of Critical Distances to estimate the static strength of notched samples of Al6082 loaded in combined tension and torsion. Part I Material cracking behaviour, *Engineering Fracture Mechanics*, 77 (2010) 452–469.
- [24] Susmel, L., Taylor, D., The theory of critical distances to predict static strength of notched brittle components subjected to mixed-mode loading, *Engineering Fracture Mechanics*, 75 (2008) 534–550.
- [25] Maggiolini, E., Livieri, P., Tovo, R., Implicit Gradient and Integral Average Effective Stresses Relationships and Numerical Approximations, *Fatigue and Fracture of Engineering Materials & Structures*, in press, doi: 10.1111/ffe.12216.
- [26] Tovo, R., Lazzarin, P., Berto, F., Cova, M., , E., Experimental investigation of the multiaxial fatigue strength of ductile cast iron, *Theoretical and Applied Fracture Mechanics*, in press, doi: 10.1016/j.tafmec.2014.07.003.